Structure and Selectivity of a Monovalent Cation Binding Site in Cubic Insulin Crystals

John Badger, Alexander Kapulsky, Olga Gursky, Balaji Bhyravbhatla, and Donald L. D. Caspar
Rosenstiel Basic Medical Sciences Research Center, Brandeis University, Waltham, Massachusetts 02254 USA

ABSTRACT Cubic insulin crystals contain a binding site for monovalent cations in a cavity on the crystal dyad in which the bound cation is ligated by protein atomic dipoles and water molecules. These types of interaction are analogous to interactions that occur in small cation-selective carrier and channel molecules. X-ray diffraction data collected from cubic insulin crystals containing Li^+, Na^+, K^+, NH_4^+, Rb^+, and Tl^+ show that (i) the differences in cation size do not cause any large alteration in the protein structure around the cation, and (ii) the bound cation is co-ordinated by one or two water molecules, depending on its ionic radii. The relative binding affinities for cations at this dyad site were obtained from an x-ray diffraction analysis of competition experiments in which crystals were dialyzed in mixtures of Tl^+ with Li^+, Na^+, K^+, NH_4^+, Rb^+, or Cs^+. These data show that this site provides very little discrimination between Na^+, K^+, Rb^+, and Tl^+, some selectivity against the small Li^+ and the tetrahedrally shaped NH_4^+, and stronger selectivity against the larger Cs^+. The capacity of this site to bind monovalent cations of different sizes may be accounted for by the small number of protein ligating groups and a change from two ligating waters with Li^+ and Na^+ to one ligating water with the larger cations.

INTRODUCTION

A functionally important characteristic of ion channels, ion carriers, and many enzymes is their ability to distinguish between different monovalent cations. Observing that the free energies of both hydrated cations and cation: host complexes are inversely proportional to their ionic radii, Eisenman has developed a successful general theory for selective ion binding (Eisenman, 1961). According to this theory, the dominant factor determining cation binding specificity is the electrostatic field strength at the site and the degree of selectivity depends on the amount of water within the site. However, only the atomic structures of relatively small molecules have been available for making detailed quantitative comparisons of cation binding interactions with experimental selectivity data (Eisenman et al., 1992; Grootenhuis and Kollman, 1989). The bound cations in the cation-selective gramicidin and valinomycin molecules are ligated by atomic dipoles rather than ionizable groups; similar interactions have been proposed for other ion channels (Eisenman and Dani, 1987).

The two sites in cubic insulin crystals at which well-ordered monovalent cations are bound (Gursky et al., 1992a, b) involve co-ordination by carbonyl oxygen dipoles and water with no involvement of negatively charged protein groups. Measurements of low-resolution anomalous scattering data from Tl^+ containing crystals have revealed diffuse localization of Tl^+ at an additional four partially ordered sites in which some or all of the ligating groups are also atomic dipoles (Badger et al., 1993). The identification of these monovalent cation binding interactions is of interest because, in contrast to the variety of binding sites that have been identified for divalent cations (Chakrabarti 1990a, b), only a few monovalent cation binding sites have been identified in protein crystal structures (Pantoliano et al., 1988; Gros et al., 1989; Toney et al., 1993).

In previous work we showed that a small cavity between two protein molecules related by the crystal dyad in cubic insulin creates one binding site for any one of the monovalent cations Li^+, Na^+, K^+, Rb^+, and Tl^+ (Gursky et al., 1992a). X-ray diffraction data collected from Tl-insulin and Na-insulin crystals at 0.1 M ionic strength showed that this cavity contains a single asymmetrically located monovalent cation with an occupancy of > 0.9 at pH > 9.5. According to high resolution x-ray crystallographic refinements of Na-insulin crystals (Gursky et al., 1992b) and energetic considerations (Badger, 1993), the bound Na^+ is tetrahedrally co-ordinated by the main chain carbonyls of A5 Gln and A10 Val and *two* water molecules (one additional water to the model originally proposed (Gursky et al., 1992a)). In crystals dialyzed with 0.1 M Na^+ at pH 7 this site contains water molecules but no cation and the side chains of A5 Gln and A9 Ser, which enclose the cation binding cavity at higher pH, rotate into different orientations to open up the water-filled cleft across the dyad. Although occupation of this cavity site by monovalent cations depends on the charge on the titratable amino acids in the protein, the site does not contain any ionizable groups.

In this report we describe an analysis of x-ray diffraction data leading to atomic models of the Li^+, K^+, NH_4^+, Rb^+, Tl^+, and associated waters bound at the dyad site. In order to determine the specificity of this site for these monovalent cations we have also measured diffraction data from crystals equilibrated with mixtures of each cation with the more strongly scattering Tl^+. By comparing the relative amounts of Tl^+ in the dialyzing solutions with the crystallographically determined occupancies of Tl^+ near the crystal dyad, we have obtained a selectivity series that includes all of these

Received for publication 6 July 1993 and in final form 15 November 1993
Address reprint requests to John Badger

0006-3495/94/02/286/07 $2.00

cations. This method for determining the binding selectivity between two competing ligands can be generally useful when one ligand is a much stronger scatterer than the other. In contrast to chemical or radioactive methods for measuring competitive binding, which can be complicated by the presence of other binding sites on the protein, this crystallographic approach allows a direct determination of competitive binding at the specific site of interest.

MATERIALS AND METHODS

Crystal preparation and data collection

Crystallization conditions, dialysis procedures and data collection from bovine cubic insulin crystals in 0.1 M Li^+, Na^+, K^+, Rb^+, and Tl^+ at pH 9 have been described previously (Gursky et al., 1992a). The bovine and porcine cubic insulin crystals used to measure the new data reported in this paper were grown in the same way. Before dialyzing crystals in mixtures of monovalent cations, the crystals were placed in 0.1 M Na^+ acetate/carbonate solution at pH 9.5–10 overnight. This was done in order to remove the phosphate used in the crystallizations, which forms relatively insoluble salts with some of the monovalent cations. Crystals were then dialyzed in mixtures Li^+/Tl^+, Na^+/Tl^+, NH_4^+/Tl^+, K^+/Tl^+, Rb^+/Tl^+, Cs^+/Tl^+, Li^+/Cs^+, and Na^+/Cs^+ carbonate salts at a total ionic strength of 0.1 M at pH 9.5–10. The ionic radii and number of electrons of the cations used in this study are listed in Table 1. A concentration of 0.1 M in monovalent cations was chosen for these experiments, because previous work (Gursky et al., 1992a) showed that the crystals are not stable at lower ionic strength.

Diffraction data for the selectivity analysis were collected on the Brandeis TV area detector (Kalata, 1985; Kalata et al., 1990). Most sets of data were collected over a single rotation of 90° in 0.1° frames. The risk of introducing systematic errors when scaling together different sets of data was avoided by collecting all the diffraction data for a given solvent condition from one crystal in a single detector run. Data were usually collected to 2.8-Å resolution, because the higher resolution data at pH 9.5–10 was generally of poor quality, particularly in crystals where more than 1/3 of the monovalent cations were Tl^+. Data collection and initial processing was carried out using the MADNES program (Pflugrath and Messerschmidt, 1987). Data were then corrected for crystal absorption and radiation damage (Kabsch, 1988) (Table 2).

Refinement of atomic models

The atomic co-ordinates for porcine Na-insulin refined at 1.7-Å resolution (Badger et al., 1991) and bovine Na-insulin refined at 2.0-Å resolution (Gursky et al., 1992b) were used to provide initial models for cubic insulin crystals containing Li^+, K^+, NH_4^+, Rb^+, and Tl^+. Bovine and porcine insulins differ only by conservative substitutions A8 Thr>Ala and A10 Ile>Val, involving side chains outside the cation binding cavity. The previously measured 2.8-Å resolution diffraction data from bovine insulin crystals that contained pure salts of Li^+, K^+, Rb^+, and Tl^+ (Gursky et al., 1992a)

TABLE 1 Ionic radii and number of scattering electrons for the monovalent cations used in the experiments reported in this paper

Cation	Ionic radii	No. of scattering electrons
	Å	
Li^+	0.76	2
Na^+	1.02	10
K^+	1.38	18
NH_4^+	1.47	10
Tl^+	1.50	80
Rb^+	1.52	36
Cs^+	1.67	54

TABLE 2 Crystallographic data collected from cubic insulin crystals in 0.1 M solutions of monovalent cations at pH 9.5–10

Insulin crystal	No. of data	No. of unique data	R_{merge}	Res
				Å
Bovine 0.70 Tl^+/0.30 Cs^+	8401	2151	6.6	2.8
Bovine 0.50 Tl^+/0.50 Rb^+	8564	2233	6.1	2.8
Bovine 0.50 Tl^+/0.50 NH_4^+	5760	1909	5.6	2.8
Porcine 0.50 Tl^+/0.50 K^+	5712	1531	8.6	2.8
Porcine 0.30 Tl^+/0.70 Na^+	16440	5429	6.5	2.0*
Porcine 0.50 Tl^+/0.50 Na^+	14936	5134	6.8	2.0*
Bovine 0.30 Tl^+/0.70 Li^+	5081	1642	5.8	2.8
Bovine 0.30 Cs^+/0.70 Na^+	7706	1921	6.7	2.8
Bovine 0.30 Cs^+/0.70 Li^+	5551	1398	7.6	2.8
Bovine NH_4^+				
(run 1)	4409	1548	5.8	3.3
(run 2)	18029	4816	8.9	2.0‡

The NH_4-insulin data was collected in two runs from the same crystal with a merging R factor of 5.5% to give a total of 4837 unique data.
* These data are relatively poor beyond 2.8 Å resolution.
‡ These data are poor beyond 3.0 Å resolution.

were used to obtain models of the cation binding sites for these cations. These data were recorded from crystals at pH 9, where cation occupancy near the crystal dyad is slightly less than unity, because the crystals at pH 9 generally gave better quality data than crystals at pH 10.

Each set of Li^+, K^+, NH_4^+, Rb^+, and Tl^+-insulin structure factor data, F_{obs}, was used to calculate a difference Fourier map with coefficients $(F_{obs} - F_{calc})\exp i\alpha$. The structure factor amplitudes, F_{calc}, and phases, α, were obtained from the Na-insulin model with the contents of the cation-binding cavity (the Na^+, two Na^+-ligating waters and one mobile water) deleted. These maps were used to make a visual analysis of electron density within the cation binding site. No significant difference density (i.e., large features exceeding 4 × the rms difference density) was observed outside of the cation binding sites in any of these maps, showing that the type of cation that is bound does not greatly alter the surrounding protein structure. For this reason, we concentrated on modeling the cation and water molecules at the localized cation binding sites. Because the ~2.8-Å resolution of the available data from these derivative crystals is relatively low, and isomorphous crystals containing Na^+ have already been refined at higher resolution (Badger et al., 1991; Gursky et al., 1992b), we considered that full structure refinement calculations would not provide any reliable additional information on the protein structure.

Phased heavy atom refinement methods (Dickerson et al., 1968) were used to determine initial positions for the heavy cations in the crystals dialyzed in pure salts and to obtain the Tl^+ occupancies in the selectivity analysis. In the refinement of the positions of the strongly scattering cations (K^+, Rb^+, Tl^+), refinement cycles in which the cation co-ordinates were adjusted were alternated with cycles in which scale factors (a multiplier and an artificial temperature factor) between F_{obs} and F_{calc} were recalculated. The scaling temperature factors did not exceed ± 8 $Å^2$ for the K^+, Rb^+, or Tl^+-containing crystals. Since long-range disorder does *not* significantly alter crystallographically refined temperature factors (Clarage et al., 1992), this result suggests that the loss of intensity data at high resolution is caused by long-range lattice disorder in the derivative crystals. After refining the positions of the strongly scattering bound cations, we then attempted to include the cation-ligating water molecules in the models. Initial trials showed that stereochemically reasonable positions of the cation-ligating water molecules could not be obtained without imposing restraints between the water molecules and their co-ordinating groups. For this reason, we modeled the bound waters using stereochemically restrained refinement methods (Hendrickson, 1985) with a program incorporating a FFT algorithm for fast computation of structure factors (Agarwal, 1978). Harmonic bond-length restraints were placed between the water molecules and selected atoms (see the main text for details). This method was also used for the entire refinement of the Li-insulin and NH_4-insulin structures since scattering from

these cations is less than or equal to scattering from the water molecules. The refinements of all of these models against data in the resolution range 10–2.8 Å terminated with R values of 0.21.

For the Tl^+ occupancy determinations at the dyad site in the crystals dialyzed with mixtures of Tl^+ and other cations, initial structure factors were calculated from models for each cation and associated waters with the cation occupancies set equal to the fraction in the dialyzing solutions. The temperature factor of the Tl^+ was set to 20 $Å^2$ and only the Tl^+ occupancy and scale factor between F_{obs} and F_{calc} were treated as variables. Because the available structure factor data extend to only 2.8-Å resolution, the refined Tl^+ occupancy is not very sensitive to the exact value of the temperature factor used. Fixing the Tl^+ temperature factor at a reasonable value gives a better determined solution in the occupancy factor refinement than allowing the temperature factor to change. In previous work, in which we carried out similar refinements of Tl^+ occupancies, we obtained good correlations between pH-dependent changes in Tl^+ occupancies (Gursky et al., 1992a; Badger et al., 1993) and pH-dependent structural changes determined from high resolution electron density maps (Gursky et al, 1992b). Furthermore, the Tl^+ occupancies presented in this paper are all physically reasonable. These results support the validity of this refinement protocol and the choice of the value for the fixed temperature factor of the bound Tl^+ in the cavity on the crystal dyad.

The position of a second ordered Tl^+ overlaps a partially occupied conformation of B10 His and the Tl^+ occupancy at this site and is very sensitive to pH between pH 9 and 10 (Gursky et al., 1992a; Badger et al., 1993). For these reasons the Tl^+ occupancy near B10 measured at ~pH 9.5 is variable, depending on the exact pH of the crystals. Because this site involves coordination by only two carbonyl dipoles at the protein surface, it would not be expected to show significant selectivity for the monovalent cations. Therefore the fractional Tl^+ occupancy modeled at this site in the mixed cation solutions was fixed at the proportion in the solvent. The four disordered Tl^+ binding sites identified from anomalous scattering measurements (Badger et al., 1993) require careful measurement and scaling of low-resolution diffraction data (d > 10 Å) to be detected and so were also excluded from this analysis.

RESULTS

Ligation of bound cations

(i) Li- and Na-insulin

In the difference Fourier omit map calculated from the Li-insulin crystal data at pH 9, the only features stronger than 4 × the rms density fluctuation are two connected lobes of density at the cation binding site near the dyad and, deeper within the cavity, a weak feature. The weak density feature is close to the position of a mobile water molecule in the Na-insulin structure (Badger et al., 1991; Gursky et al., 1992b; Badger, 1993) and is accounted for by a similar water molecule in the Li-insulin crystal. The stronger two-lobed feature can be interpreted in the same way as in the Na-insulin structure (Gursky et al., 1992b; Badger, 1993), where the cation is tetrahedrally co-ordinated by the main chain carbonyl atoms of A5 Gln and A10 Val and ligated by two water molecules. Because the asymmetric Li^+:$2H_20$ cluster is centered on a crystal dyad the corresponding electron density overlaps with the electron density from a symmetry-related cluster. This fact, together with the limited resolution of the diffraction data and the small scattering factors of the Li^+ and waters, precludes meaningful crystallographic refinement of these atoms without stereochemical restraints.

Model co-ordinates for the Li^+:$2H_20$ cluster were obtained by positional refinement of these atoms with bond-length restraints between the Li^+ and its four ligating atoms (Fig. 1). These co-ordinates are given in Table 3. This model and the high resolution Na-insulin structure (Gursky et al., 1992b) suggest that one water is a hydrogen donor to the main and side chain atoms of A5′ Gln and a hydrogen acceptor from the side chain of A9′ Ser (′ denotes an atomic group related by the crystal symmetry to the reference molecule). The second cation-ligating water could be hydrogen-bonded to the side chain oxygen of A5 Gln and the main chain carbonyl of A10′ Val. Because the side chain of A15 Gln is somewhat disordered (described by multiple conformations or high temperature factors in the refined 2-Å resolution Na-insulin models (Gursky et al., 1992b)), it is unclear if this side chain forms additional specific stabilizing interactions with either of the two cation-ligating water molecules. A plausible model has the side chain amide group of A15 Gln forming a hydrogen bond with this second water molecule (Fig. 1). The differences in the co-ordinates of the cation-ligating water molecules in the Na-insulin structure (Gursky et al., 1992b) and the Li-insulin structure are due to the smaller radius of the Li^+, which allows a closer approach the ligating carbonyl groups and a closer approach by the ligating waters.

(ii) K-, NH_4-, Rb-, and Tl-insulins

Difference Fourier omit maps computed from data for the larger cations with ionic radii between 1.38 and 1.52 Å, show a strong feature smeared across the crystal dyad. All these maps also show weak but significant density at the position of the mobile water molecule on the dyad axis identified in the Li- and Na-insulin structures. The strong difference density in these maps is fitted by a cation that ligates the main chain carbonyl atoms of A5 Gln and A10 Val (as for Li^+ and Na^+) and, because these cations have larger radii than Li^+ or Na^+, the side chain oxygen of A5 Gln. In these structures there is only sufficient space for one water molecule. Because the ionic radii of these cations and a water molecule are similar, the position of the ligating water would be close to the symmetry-related cation site across the local crystal dyad (Gursky et al., 1992b). To confirm the presence of this water molecule, trial occupancy refinements were carried out with the NH_4-insulin data. For NH_4-insulin, we have measured data at pH >9.5, when the NH_4^+ should be present with unit occupancy, and the amount of scattering from this ligating water is comparable to scattering from the NH_4^+. Assuming temperature factors of 20 $Å^2$ (similar to most protein atoms in the structure), the refinement gave unit occupancy factors for the NH_4^+ and a ligating water molecule placed in the symmetry-related site across the crystal dyad.

Positions for the strongly scattering cations (K^+, Rb^+, Tl^+) were initially refined using phased heavy atom refinement methods (Dickerson et al., 1968). Refinements of the cations and waters were then continued with bond restraints placed between the water molecules and the cation and protein ligating groups. These refined models are exemplified by the K-insulin structure shown in Fig. 2. The co-ordinates for the bound cations and associated water in these three structures are very similar within small variations caused by their

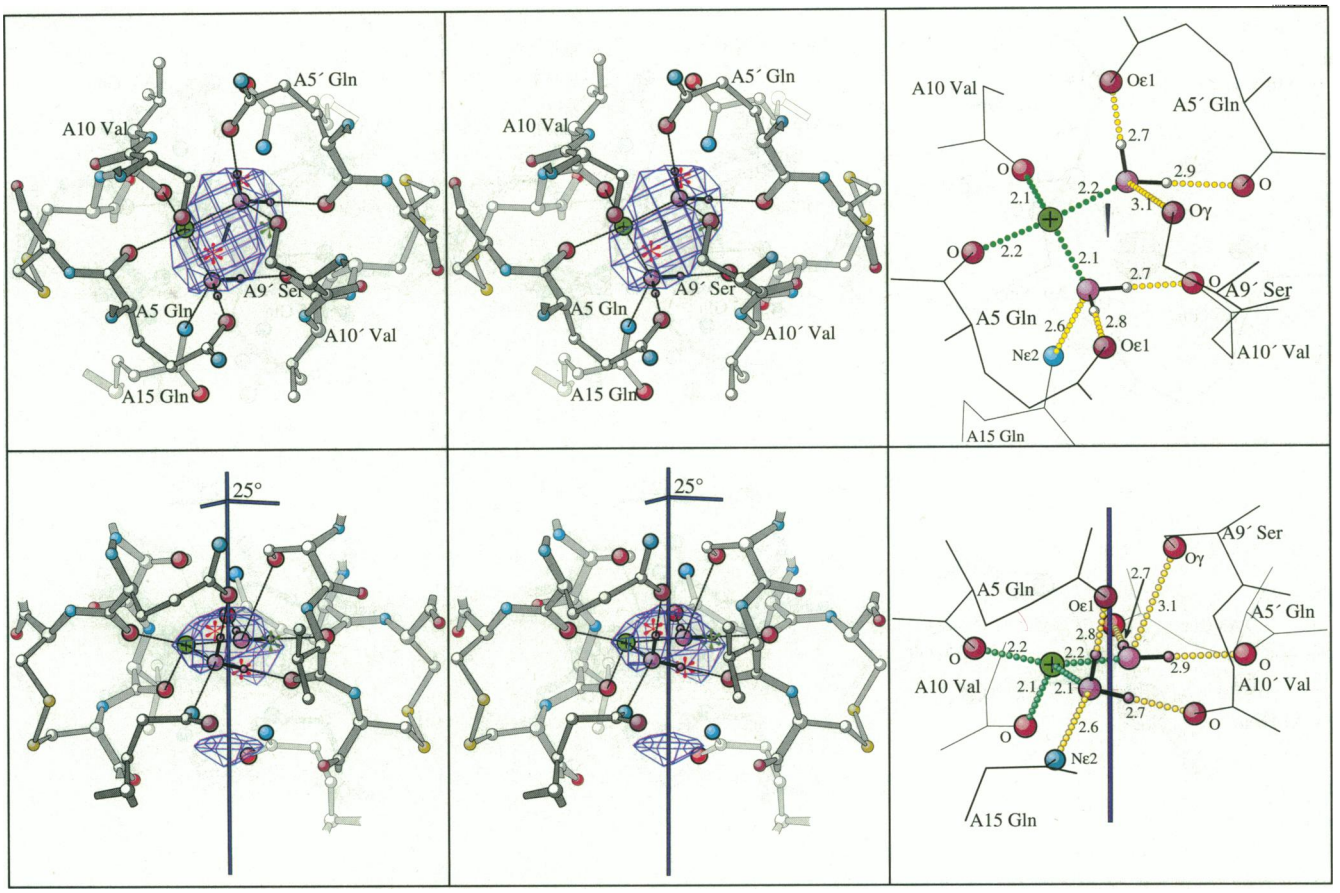

FIGURE 1 Binding of the lithium ion and two water molecules in the electronegative dipolar cavity located on the twofold axis of the cubic insulin crystals. The stereopair illustration shows orthogonal views of the sequence A5 Gln.A6Cys...A9 Ser.A10 Val.A11 Cys...which forms the cavity. (Protein oxygen: *red*, nitrogen: *cyan*, sulfur: *yellow*, water oxygen: *magenta*, and lithium: *green*; residues interacting with the cavity contents are labeled, with primes for the segment to the right of the dyad which is tilted away from the vertical by 6°). Superimposed in blue is the 2.8-Å resolution difference electron density map calculated from the Li-insulin crystal data and model structure factors for the protein with the cavity contents omitted. The orthogonal diagrams at the right indicate the bond distances for the co-ordination of the Li ion and two water molecules in a model adjusted to fit the difference electron density maps with plausible hydrogen bonding and cation-oxygen distances. Atomic co-ordinates for the protein were taken from the model refined to fit the 2-Å resolution data for Na-insulin (Gursky et al., 1992b) with imposition of strict twofold symmetry at the dyad axis. Because the contents of the cavity do not have twofold symmetry, the protein structure on either side of the dyad cavity may vary slightly depending on the orientation of the ion and water. In the stereo diagrams, the alternate symmetry related configuration of the ion and water are starred. The dipolar groups lining the ion binding cavity are the pairs of A5 and A10 peptide carbonyls, the A5 and A15 glutamine side chains and the A9 serine hydroxyls. Depending on their orientations, the hydroxyls and amides can serve as proton donors for hydrogen bonding the water. With two water molecules and one cation in the cavity, two proton donors from the protein are required to complete the tetrahedral co-ordination of the water molecules. In the model, A9′ Ser and A15 Gln are oriented to hydrogen bond to the negative water dipoles, but other combinations of the dipolar groups can also fit the data. The glutamines and hydroxyl not involved as proton donors for hydrogen bonding to water will be preferentially oriented with their negative dipoles pointing into the cavity to provide additional stability for the bound cation.

slightly differing ionic radii and the limitations of the experimental data. The likely hydrogen acceptors for the water in these structures are any one of the three possible pairs of the three oxygen atoms from the main chain and side chain atoms of A5′ Gln and A9′ Ser. It is unclear if the side chain of A15′ Gln provides additional stabilizing interactions for this water or if A15 Gln is oriented so as to make significant interactions with the bound cation.

(iii) Cs-insulin

Crystals dialyzed in 0.1 M Cs^+ shatter within 1 h, preventing the collection of diffraction data (Gursky et al., 1992a). However, crystals dialyzed in 0.1 M Na^+/Cs^+ and 0.1 M Li^+/Cs^+ remained stable when Cs^+ comprised <1/3 of the number of monovalent cations in the dialyzing solution. Difference Fourier maps computed from these data failed to show any indication of Cs^+ and contained features very similar to Li-insulin and Na-insulin crystals. Model-building trials show that a rigid cavity with the dimensions found for the smaller cations is too small to accommodate a Cs^+ and ligating water in the same type of arrangement as modeled for the K-, NH_4-, Rb-, and Tl-insulins. However, an alternative arrangement, with the Cs^+ in the center of the cavity and the water absent, would fit within the available volume in this cavity. Thus, the absence of observable Cs^+ binding at this site is not due to the steric restraints of the cavity.

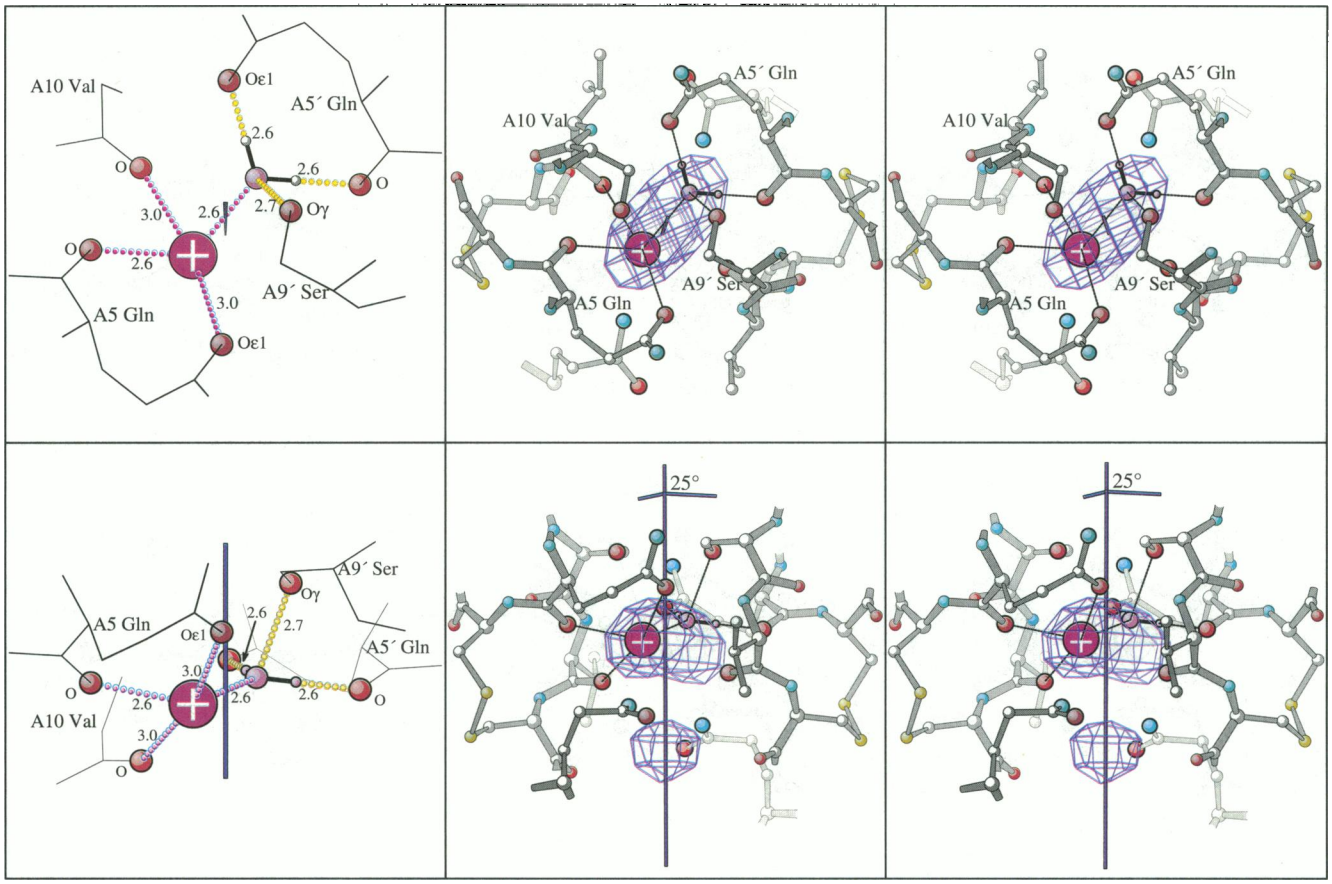

FIGURE 2 Binding of a potassium ion and one water molecule in the electronegative dipolar cavity located on the twofold axis of the cubic insulin crystal. The orthogonal stereopair illustrations and co-ordination diagram (left) are drawn as in Fig. 1, with the potassium ion colored purple. The water molecule is shown forming hydrogen bonds with the A5 peptide carbonyl and the side chains of A9 Ser and A5 Gln. Since the x-ray diffraction data do not allow a distinction to be made between the =O and —NH_2 groups in the A5 Gln side chain, or identification of the hydrogen position in the A9 Ser side chain, either one of these side chains could be the hydrogen donor for the water. Only very small variations in atomic co-ordinates are needed to allow this cavity to accommodate ions that range in size between Li^+ and Tl^+ and a change from two ligating waters in the case of Li^+ or Na^+ to one ligating water for the larger cations. Figs. 1 and 2 were drawn with the MOLSCRIPT program (Kraulis, 1991) as modified by E. Fontano.

Crystallographic determination of cation binding selectivity

The x-ray diffraction data (Table 2) collected from crystals dialyzed with the 0.1 M of Tl^+/Li^+, Tl^+/Na^+, Tl^+/K^+, Tl^+/NH_4^+, Tl^+/Rb^+ and Tl^+/Cs^+ were analyzed to determine the Tl^+ occupancies at the localized cation binding site. Comparisons of the relative amounts of Tl^+ in the dialyzing solution and the observed occupancy within the cavity directly measure the selectivity of this particular cation binding site. Models were constructed that contained the lighter cations and associated waters with occupancies equal to the fraction of these cations in the dialyzing solution. The Tl^+ occupancies at the previously determined sites were then refined (Dickerson et al., 1968) against the x-ray data between 10- and 2.8-Å resolution with the Tl^+ temperature factor fixed at 20 $Å^2$ (Table 4). Test refinements showed that the occupancies assumed for Li^+, Na^+, NH_4^+, and K^+ in these calculations had very little effect on the refined Tl^+ occupancies, because scattering is dominated by the Tl^+. For refinements with Rb^+ and Cs^+ there is greater uncertainty in the occupancy of the bound Tl^+, but the data still limit the possible range of occupancies for these cations.

The refined Tl^+ occupancies show that the ratios of Na^+/Tl^+, K^+/Tl^+, and Rb^+/Tl^+ at the localized binding site are very similar to the ratios of these cations in the corresponding dialyzing solutions. The two sets of Na^+/Tl^+ measurements, made from crystals containing different amounts of bound Tl^+, are consistent with the compositions of the dialyzing solutions, showing that these experimental and computational methods are reliable. Although Tl^+ is more polarizable than Rb^+, it might be expected that the similar sizes of Rb^+ and Tl^+ would lead to similar binding affinities at this site and the refined occupancies are consistent with this assumption. Based on these comparisons the estimated uncertainty in the fractional Tl^+ occupancy values is ~0.1. Thus, within this estimate of experimental accuracy, there is no detectable selectivity at this site between Na^+, K^+, Rb^+, and Tl^+. The data from crystals containing Li^+/Tl^+ and NH_4^+/Tl^+ show that the small Li^+ and the tetrahedrally shaped NH_4^+ binds slightly less well than Tl^+. As previously noted, no Cs^+ was observed in difference maps computed from crystals containing mixtures of Li^+/Cs^+ and Na^+/Cs^+. Refinements of the Tl^+ occupancy using the data from the Cs^+/Tl^+ crystal and using a model structure that contained

TABLE 3 Atomic co-ordinates (space group I2,3, unit cell dimension, a = 78.9 Å) for the bound cations and ligating waters

Structure		Co-ordinates		
		X	*Y*	*Z*
Li^+:2H_2O	Li^+	0.64	3.56	−1.30
	H_2O	0.67	3.82	0.85
	H_2O	−1.31	2.77	−1.17
Na^+:2H_2O	Na^+	0.47	3.86	−1.11
	H_2O	0.81	3.91	1.17
	H_2O	−1.71	3.12	0.00
K^+:H_2O	K^+	−0.49	3.35	−1.13
	H_2O	0.55	4.23	1.12
NH_4^+:H_2O	NH_4^+	−0.89	3.71	−1.01
	H_2O	0.67	3.61	1.17
Rb^+:H_2O	Rb^+	−0.63	3.42	−1.18
	H_2O	0.55	4.18	1.12
Tl^+:H_2O	Tl^+	−0.44	3.36	−0.98
	H_2O	0.61	4.23	1.25

Values are given in angstroms relative to a point on the twofold (*y*) axis with fractional co-ordinates (1/4, 1/2, 1/2). The *x* and *z* axes are parallel to the nonintersecting crystal dyads that are symmetry-related to the *y* axis (cf. Figs. 1 and 2). The co-ordinates for the Na^+:2H_2O are those previously obtained from refinement at 1.9-Å resolution without stereochemical restraints (Gursky et al., 1992b). Stereochemically accurate co-ordinates for the Li^+ and for the water molecules in the other structures could not be obtained from the 2.8-Å resolution data alone and were determined with bond-length restraints for the water molecules.

TABLE 4 Fractional occupancies of Tl^+ in cubic insulin crystals dialyzed in mixtures of Tl^+ with other cations

Fractional composition of soaking solution	Fractional Tl^+ occupancy per dyad	Fractional difference between bound and free Tl^+
0.67 Tl^+/0.33 Cs^+	0.93	+0.24
0.5 Tl^+/0.5 Rb^+	0.43	−0.07
0.5 Tl^+/0.5 NH_4^+	0.75	+0.25
0.5 Tl^+/0.5 K^+	0.53	+0.03
0.5 Tl^+/0.5 Na^+	0.49	−0.01
0.3 Tl^+/0.7 Na^+	0.39	+0.09
0.33 Tl^+/0.67 Li^+	0.68	+0.34

The occupancies are given for each cation binding cavity. There are two closely spaced sites related by the dyad, only one of which may be occupied. Previously occupancies were designated as the average at each site (Gursky et al., 1992a, b; Badger et al., 1993). The difference between the fractional occupancy of Tl^+ in the dyad cavity obtained from crystallographic refinements and the amount of Tl^+ in the crystal solvent is given in the third column. This value would be zero for stoichiometric (unselective) binding. Except for the Cs^+-containing structure, in which the Cs^+ occupancy was initially assumed to be zero, the occupancies for the cations were initially assumed to correspond to the compositions of the soaking solution.

no Cs^+, gave a Tl^+ occupancy of 0.93 per dyad (Table 4), which is consistent with an absence of Cs^+ from this site.

DISCUSSION

Cation binding structure

All the monovalent cations that we have investigated are able to fit into the cation binding cavity observed in Na-insulin crystals but the cavity volume restricts the number of ligating waters. This cavity is observed to accommodate monovalent cations with radii <1.5 Å and, depending on cation size, one or two ligating water molecules. The absence of significant features in the 2.8-Å resolution difference maps shows that none of these cations causes any major conformational change in the protein structure at the cation binding site. The rigidity of the backbone atoms forming the cavity is further exemplified by high resolution refinement of the Na-insulin structure at pH 7 (Gursky et al., 1992b). At pH 7 there is no cation at this site, but the carbonyl atoms of A5 Gln and A10 Val remain in almost the same positions as in the cation-containing structures. However, at pH 7 the side chain of A5 Gln is rotated away from the cavity, and the space occupied by the side chain oxygen atom is occupied by a water molecule. The side chain of A9 Ser is also found in an altered conformation at pH 7, implicating this side chain in the binding of the cation or the associated water molecules.

The co-ordination schemes for Li^+:$(H_2O)_2$ and K^+:(H_2O) illustrated in Figs. 1 and 2 satisfy the hydrogen bonding potential of the water molecules and the surrounding protein. At the resolution of the experimental data, and within the limits of the thermal fluctuations implied by the temperature factors determined from high resolution structure refinements (Badger et al., 1991; Gursky et al., 1992b), a number of slightly different arrangements of hydrogen donors and acceptors is possible. Because the contents of the cavity cannot have twofold symmetry the instantaneous structures of the symmetry related peptide segments co-ordinating the cation and water need not be identical. However, in Figs. 1 and 2 we show that a symmetric structure can accommodate realistic models of the bound cations and associated waters with only small deviations from ideal hydrogen-bond lengths. Of the amino acids in the cation-binding cavity, only the side chain of A15 Gln appears very mobile and this observed disorder could be associated with the asymmetry in the cation cavity contents.

Energetic factors determining cation binding selectivity

According to the x-ray diffraction data, the dyad-cavity site discriminates against Cs^+ binding, is slightly unfavorable for binding Li^+, and does not discriminate between Na^+, K^+, and Rb^+. These results are consistent with "Eisenman sequence VIII" Na>K>Rb>Li>Cs for describing the weak selectivity of this site (Eisenman, 1961). The small number of protein atoms directly ligating the cation and variability in the number and precise positions of water molecules associated with the bound cations may be the main factors responsible for the lack of strong selectivity at this site. A loss of selectivity in cation sites that contain water is one of the general principles of the Eisenman (1961) theory for cation selectivity. These atomic structures and selectivity measurements on the cubic insulin crystals imply that sites that contain few cation-ligating groups and one or two water molecules are not likely to be strongly cation-selective. Only very small changes in the positions of the ligating atoms are necessary for the broad specificity of this cation binding site. In particular, the glutamine and serine side chains may serve as

hydrogen donors or acceptors, depending on the number and positions of water molecules inside the cavity. Although the cation binding in the cubic insulin crystals has no functional significance in insulin activity, the plasticity of this cavity structure illustrates the potential adaptability of protein binding sites which involve very small movements to accommodate different ligands. Similarly, in Met>Ala mutations of α-lytic protease, very broad substrate binding specificity was accounted for by structural plasticity involving only ~0.1-Å movements of main chain atoms and small rearrangements of side chain orientations (Bone et al., 1989).

The x-ray diffraction analysis measured fractional occupancies for the Tl^+ at the dyad site in the cubic insulin crystal. Since the total cation occupancy per dyad is almost unity for these experimental conditions, the occupancy of the competing cation is also known from the Tl^+ occupancy determination. For equimolar dialyzing mixtures, the ratio of the Tl^+ occupancy at this site to the occupancy of the competing cation is $\exp(-\Delta G/kT)$, where ΔG is the binding free energy difference between these two cations. Thus, for estimated occupancy errors of ~0.1 these measurements are sensitive to binding free energy differences of $\sim kT/2$. An absence of selectivity between Tl^+ and other cations shows that the binding free energy differences between the various cations must be almost identical to the corresponding free energy differences between the hydrated cations. This equivalence of binding and hydration free energy differences will provide a very critical test of computational methods for calculating relative binding affinities. Free energy perturbation calculations with a carefully calibrated potential energy function were able to account for the selectivity properties of the valinomycin molecule in a quantitative way (Eisenman et al., 1992). Similar calculations on this localized cation site in cubic insulin crystals would independently test these energy parameters and give a quantitative account of the interactions responsible for cation binding.

We thank Prof. George Eisenman for providing a great deal of helpful information on ionic selectivity and useful discussions regarding these experimental results. We thank Eric Fontano for assistance with the preparation of the figures. This project was supported was by grant CA 47439 (to D. L. D. Caspar) from the National Cancer Institute. The Brandeis TV detector was developed by Ken Kalata and Walter Phillips and supported by grant BBS-8713278 from the National Science Foundation.

REFERENCES

Agarwal, R. C. 1978. A new least-squares refinement technique based on the fast Fourier transform algorithm. *Acta Crystallogr.* A34:791–809.

Badger, J., M. R. Harris, C. D. Reynolds, A. E. Evans, E. J. Dodson G. G. Dodson, and A. C. T. North. 1991. Structure of the pig insulin dimer in the cubic crystal. *Acta Crystallogr.* B47:127–136

Badger, J., Y. Li, and D. L. D. Caspar 1993. Thallium counterion distribution in cubic insulin crystals determined from anomalous x-ray diffraction data. *Proc. Natl. Acad. Sci. USA.* In press.

Badger, J. 1993. Display and interpretation of solvent density distributions in insulin crystals. *J. Mol. Graphics.* In press.

Bone, R., J. L. Silen, and D. A. Agard. 1989. Structural plasticity broadens the specificity of an engineered protease. *Nature (Lond.).* 339:191–195.

Chakrabarti, P. 1990a. Systematics in the interaction of metal ions with the main-chain carbonyl group in protein structures. *Biochemistry.* 29: 651–658.

Chakrabarti, P. 1990b. Interactions of metal ions with carboxylic and carboxamide groups in protein structures. *Prot. Eng.* 4:49–56.

Clarage, J. B., M. S. Clarage, W. C. Phillips, R. M. Sweet, and D. L. D. Caspar. 1992. Correlations of atomic movements in lysozyme crystals. *Proteins.* 12:145–157.

Dickerson, R. E., J. E. Weinzierl, and R. A. Palmer. 1968. A least-squares refinement method for isomorphous replacement. *Acta Crystallogr.* B24: 997–1003.

Eisenman, G. 1961. On the elementary atomic origin of equilibrium ionic specificity. In Symposium on Membrane Transport, and Metabolism. A. Kleinzeller, and A. Kotyk, editors. Academic Press, New York. pp. 163–179.

Eisenman, G., O. Alverez, and J. Aqvist. 1992. Free energy perturbation simulations of cation binding to valinomycin. *J. Incl. Phen. Mol. Rec. Chem.* 12:23–53.

Eisenman, G., and J. A. Dani. 1987. An introduction to molecular architecture and permeability of ion channels. *Annu. Rev. Biophys. Biophys. Chem.* 16:205–226.

Gros, P., Ch. Betzel, Z. Dauter, K. S. Wilson, and W. G. J. Hol. 1989. Molecular dynamics refinement of a thermitase-eglin-c complex at 1.98-Å resolution and a comparison of two crystal forms that differ in calcium content. *J. Mol. Biol.* 210:347–367.

Grootenhuis, P. D. J., and P. A. Kollman. 1989. Molecular mechanics and dynamics of crown ether-cation interactions: free energy calculations on the cation selectivity of dibenzo-18-crown-6, and dibenzo-30-crown-10. *J. Am. Chem. Soc.* 111:2152–2158.

Gursky, O., Y. Li, J. Badger, and D. L. D. Caspar. 1992a. Monovalent cation binding to cubic insulin crystals. *Biophys. J.* 61:604–611.

Gursky, O., J. Badger, Y. Li, and D. L. D. Caspar. 1992b. Conformational changes in cubic insulin crystals in the pH range 7–11. *Biophys. J.* 63: 1210–1220.

Hendrickson, W. A. 1985. Stereochemically restrained refinement of macromolecular structures. *Methods Enzymol.* 115B:252–270.

Kabsch, W. 1988. Evaluation of single-crystal x-ray diffraction data from a position-sensitive detector. *J. Appl. Cryst.* 21:916–924.

Kalata, K. 1985. A general purpose, computer configurable television area detector for x-ray diffraction applications. *Methods Enzymol.* 114: 486–510.

Kalata, K., W. C. Phillips, M. Stanton, and Y. Li. 1990. Development of a synchrotron CCD-based area detector for structural biology. *Proc. Soc. Photo-Opt. Instr. Eng.* 1345:270–280.

Kraulis, P. J. 1991. MOLSCRIPT: a program to produce both detailed and schematic plots of protein structures. *J. Appl. Cryst.* 24:946–950.

Pantoliano, M. W., M. Whitlow, J. F. Wood, M. L. Rollence, B. C. Finzel, G. L. Gilliland, T. L. Poulos, and P. N. Bryan. 1988. The engineering of binding affinity at metal ion binding sites for the stabilization of proteins: subtilisin as a test case. *Biochemistry.* 27:8311–8317.

Pflugrath, J. W., and A. Messerschmidt. 1987. Fast system software. In Computational Aspects of Protein Crystal Data Analysis: Proceedings of the Daresbury Study Weekend 23–24 January, 1987. J. R. Helliwell, P. A. Machin, and M. R. Papiz, editors. Science, and Engineering Research Council, Daresbury Laboratory.

Toney, M. D., E. Hohenester, S. W. Cowan, and J. N. Jansonius. 1993. Dialkylglycine decarboxylase structure: bifunctional active site and alkali metal sites. *Science (Wash. DC).* 261:756–759.